

See discussions, stats, and author profiles for this publication at: <https://www.researchgate.net/publication/50938219>

# Photoabsorption and Resonance Energy Transfer Phenomenon in CdTe–Protein Bioconjugates: An Insight into QD–Biomolecular Interactions

ARTICLE in BIOCONJUGATE CHEMISTRY · APRIL 2011

Impact Factor: 4.51 · DOI: 10.1021/bc200034a · Source: PubMed

---

CITATIONS

25

---

READS

46

## 2 AUTHORS:



Vinayaka Aaydha

Institute of Microbial Technology

19 PUBLICATIONS 214 CITATIONS

[SEE PROFILE](#)



Sarath Munna

Koneru Lakshmaiah University

8 PUBLICATIONS 53 CITATIONS

[SEE PROFILE](#)

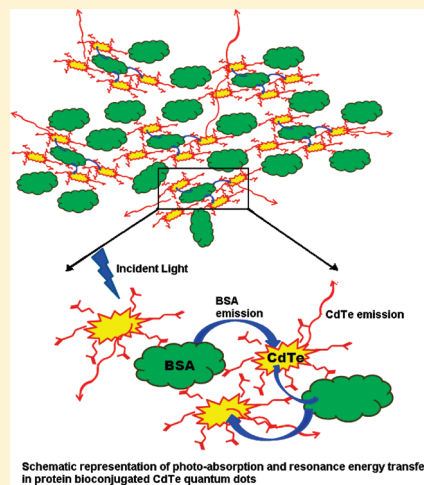
## Photoabsorption and Resonance Energy Transfer Phenomenon in CdTe–Protein Bioconjugates: An Insight into QD–Biomolecular Interactions

Aaydha C. Vinayaka and Munna S. Thakur\*

Fermentation Technology & Bioengineering Department, Central Food Technological Research Institute (A constituent laboratory of Council of Scientific and Industrial Research, New Delhi), Mysore-570020, India

 Supporting Information

**ABSTRACT:** Luminescent quantum dots (QDs) possess unique photophysical properties, which are advantageous in the development of new generation robust fluorescent probes based on Forster resonance energy transfer (FRET) phenomena. Bioconjugation of these QDs with biomolecules create hybrid materials having unique photophysical properties along with biological activity. The present study is aimed at characterizing QD bioconjugates in terms of optical behavior. Colloidal CdTe QDs capped with 3-mercaptopropionic acid (MPA) were conjugated to different proteins by the carbodiimide protocol using *N*-(3-dimethylaminopropyl)-*N*-ethylcarbodiimide hydrochloride (EDC) and a coupling reagent like *N*-hydroxysuccinimide (NHS). The photoabsorption of these QD–protein bioconjugates demonstrated an effective coupling of electronic orbitals of constituents. A linear variation in absorbance of bioconjugates at 330 nm proportionate to conjugation suggests a covalent attachment as confirmed by gel electrophoresis. A red shift in the fluorescence of bovine serum albumin (BSA) due to conjugation inferred a decrease in Stokes shift and solvent polarization effects on protein. A proportionate quenching in BSA fluorescence followed by an enhancement of QD fluorescence point toward nonradiative dipolar interactions. Further, reduction in photobleaching of BSA suggests QD–biomolecular interactions. Bioconjugation has significantly influenced the photoabsorption spectrum of QD bioconjugates suggesting the formation of a possible protein shell on the surface of QD. The experimental result suggests that these bioconjugates can be considered nanoparticle (NP) superstructures for the development of a new generation of robust nanoprobes.



### INTRODUCTION

A quantum dot is a crystal of semiconductor material (periodic groups II–VI, III–V, or IV–VI elements) with a diameter on the order of the compound's exciton Bohr radius.<sup>1</sup> They display a characteristic size dependence of their electronic and optical properties due to a phenomenon known as quantum confinement effects. Properties such as high emission quantum yield, sharp emission spectra, broad absorption spectra, chemical and photostability, long lifetimes, and tunability of emission frequencies make them a superior tool as biomarkers for various applications.<sup>2</sup> The development of any QD-based biosensing modality would essentially require the generation of bioactive QD conjugates. The coupling of inorganic nanoparticles with biomolecules generates hybrid particles possessing unique photophysical properties along with biological activity.<sup>3,4</sup> Being novel constructs, such conjugates need to be characterized to understand the full range of their modified properties before they can be utilized for biosensor applications.

Forster resonance energy transfer (FRET) is a distance-dependent nonradiative energy transfer between the excited electronic states of fluorescent molecules. This phenomenon is

a useful tool to study molecular dynamics such as biomolecular interactions and conformational changes.<sup>5</sup> The unique properties of QDs suggest that the replacement of organic fluorophores in FRET studies with QDs could lead to an experimental setup, which would be ultrasensitive, economical, and easy to configure, as well as provide the capability to make simultaneous measurements of different macromolecular systems.<sup>6</sup> Two-color organic/inorganic fluorophores are currently being used for coincidence detection based on FRET.<sup>6,7</sup> However, their functional limitations, such as the spectral cross-talk, nonuniform fluorophore photobleaching rates, and significant background fluorescence make subsequent quantification complicated. These limitations can be obviated by QDs, which have broad excitation and size-tunable photo luminescence spectra with narrow emission bandwidth, exceptional photochemical stability, and relatively high quantum yield. Further, the target signal can be amplified through enhanced energy-transfer efficiency by increasing the

**Received:** January 19, 2011

**Revised:** February 23, 2011

**Published:** April 01, 2011

number of acceptors linked to a donor. These features should allow QD-FRET-based nanosensors to generate a very distinct target signal effectively. QDs offer several advantages when used as FRET donors in place of organic dyes.<sup>8</sup> Their size-tunable and narrow emission spectra can considerably reduce donor spectral leakage into the acceptor channel. At the same time, their broad absorption spectrum at wavelengths to the blue of their emission allows choice of excitation that corresponds to the acceptor absorption minimum, substantially reducing direct excitation. QDs are expected to significantly improve assay performances in a wide variety of sensing schemes.

Although the interactions between QDs and biological molecules are known, complete characterization of such bioconjugates to understand the full range of their modified properties for biosensing applications has not been explored properly. The correlation between photoabsorption and resonance energy transfer phenomena in CdTe protein complexes has not been explored completely. The present work is aimed at characterizing QD bioconjugates based on the photoabsorption and other optical properties for the development of novel FRET-based biosensing formats. Thus, coupling the superior optical properties of QDs with a separation-free and immobilization-free FRET-based format may revolutionize the generation of robust nanobiosensors in the future.

## ■ EXPERIMENTAL SECTION

**Materials and Instruments.** Cadmium acetate [Cd(CH<sub>3</sub>COO)<sub>2</sub>], MPA, propionic acid (PA), sodium borohydride (NaBH<sub>4</sub>), tellurium, N-(3-dimethylaminopropyl)-N-ethylcarbodiimide hydrochloride (EDC), N-hydroxysuccinimide (NHS), BSA, streptavidin (SA), alkaline phosphatase (ALP), and horseradish peroxidase (HRP) were procured from Sigma Chemicals, St. Louis, USA. All reagents used were of analytical grade and acquired from standard suppliers. Dialysis membranes having 6–8 kDa molecular weight cutoff and 1 kDa molecular weight cutoff were procured from Spectra/Por, USA. The following instruments were used: UV-vis spectrophotometer (UV-1601, Shimadzu, Japan), spectrofluorimeter (RF-5301 PC, Shimadzu, Japan), transmission electron microscope (Jeol 2100, USA). Samples were analyzed using a 400-mesh carbon grid obtained from Pacific Grid Technology (101 California Street, San Francisco, CA 94111, USA).

**Synthesis of CdTe Qds.** CdTe QDs of different fluorescent emission spectra (CdTe 523, 557, 573, 601, and 640 nm) were synthesized as reported by Li et al. (2007) with modification.<sup>9</sup> In brief, 25 mL of aqueous solution containing 0.02 M Cd(CH<sub>3</sub>COO)<sub>2</sub> was mixed with 0.05 M of MPA, and the solution was degassed followed by adjusting the pH to 9.2. In a separate reaction, sodium hydrogen telluride (NaHTe) was synthesized by reacting 0.03 M of NaBH<sub>4</sub> and 0.01 M of Te in ice-cooled water and purged with argon gas for 30 min. The metal dissolved, leaving a faint pinkish-colored solution. A few drops of NaHTe were added dropwise to the above synthesized solution until the solution turned orange. The solution was refluxed for 120 min. Transmission electron microscopy (TEM) determined the size of thus-synthesized QDs. These QDs were bioconjugated to different biomolecules as explained below.

**Bioconjugation of QDs.** The following two-step protocol was used for the conjugation of QD to primary amine-containing biomolecules.<sup>10</sup> 0.05 M EDC and 5 mM NHS were mixed and the pH adjusted to 7.4, followed by incubating with QD solution in PBS at 32 °C for 15 min at 110 rpm. The protein solution in

PBS was added to the reaction mixture and further incubated at 32 °C for 150 min at 110 rpm. The solution was then kept at 4 °C overnight to deactivate the remaining EDC-NHS. The conjugate solution was then dialyzed against PBS using Spectra/Por dialysis membranes of 6–8 kDa cutoffs with 4 changes of buffer.

A standard protein, BSA, was conjugated to four different QDs to observe the difference in their conjugation efficiency. 50 μL aliquots of QD<sub>523</sub>, QD<sub>557</sub>, QD<sub>573</sub>, QD<sub>601</sub>, and QD-GSH in PBS were conjugated separately with 1 mg of BSA in 1000 μL by the above-mentioned EDC/NHS conjugation protocol.

Further, conjugation was also performed between varying concentrations of BSA in the first set of experiments keeping the QD concentration constant. 50 μL aliquots of QD<sub>557</sub> in PBS were conjugated separately with 50, 100, 250, 500, 1000, and 2000 μg of BSA in 1000 μL by the EDC/NHS protocol. In the second set, the conjugation was performed between varying concentrations of QD (5, 10, 20, 50, 100, and 150 μL of QD<sub>557</sub> in 1000 μL PBS) keeping the BSA concentration constant (50 μg) by the EDC/NHS protocol. In the third set of experiments, QD<sub>557</sub> was conjugated with other proteins to formalize the results obtained with BSA conjugates. 50 μL of QD<sub>557</sub> in PBS was conjugated separately with 50, 100, 250, and 500 μg of SA, ALP, and HRP sequentially in 1000 μL of PBS by the EDC/NHS protocol.

**Absorption Spectrometry.** The conjugates were subjected to spectrophotometry to probe the changes in the spectral properties of the conjugates due to the interfacing of inorganic nanoparticles with biomolecules. The absorbance spectra of QD bioconjugates were acquired in two ways: by restricting the protein concentration to 50 μg/mL and by restricting the QD concentration to 5 μL/mL.

**Fluorescence Spectrometry.** The influence of bioconjugation on QD photoluminescence (PL) was studied through fluorimetry. Fluorescence spectra were taken for QD-BSA conjugates restricting the protein concentration at 5 μg/mL and restricting the QD concentration at 2 μL/mL. The emission spectra were generated at the excitation wavelengths of 280, 320, and 350 nm in separate experiments. The excitation at 280 nm leads to excitation of both protein and QD components, while the excitation of 320 and 350 nm excites only the QD component of the conjugate.

Time course fluorescence of standard BSA and BSA-QD<sub>557</sub> conjugate samples were obtained by monitoring emission ( $\lambda_{em}$ ) at 350 nm for BSA component and 557 nm for QD<sub>557</sub> component with excitation at 280 nm. This method was used for the calculation of photobleaching time and FRET efficiency.

**Native PAGE.** Native-PAGE analyses of QD–protein conjugates was performed to confirm bioconjugation and to monitor the effects of CdTe QD on the mobility of proteins under electric field. The electrophoresis was run on 10% separating gel and 5% stacking gel by the protocol described by Laemmli. To observe the difference in mobility of the conjugates, the gel was stained with silver nitrate stain.

## ■ RESULTS AND DISCUSSION

**Synthesis and Bioconjugation of CdTe QDs.** Thiol-stabilized CdTe QDs were synthesized by aqueous method to attain biocompatibility, which was the primary criterion necessary for bioconjugation. In aqueous method, synthesis of colloidal nanoparticles generally depends on the molar concentrations of precursors and capping material at a particular temperature.

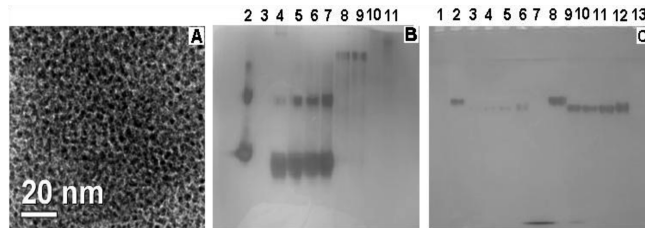


**Figure 1.** (A) Transmission electron micrograph of MPA capped CdTe QD ( $\text{QD}_{557}$ ) taken on TEM Jeol 2100, USA, at 200 KV using 400 mesh carbon copper grid from pacific grid technology. (B) Native PAGE analysis of  $\text{QD}_{557}$  conjugates of BSA, ALP, and HRP. Standard BSA, ALP, and HRP were loaded on wells 2, 8, and 10, respectively. BSA- $\text{QD}_{557}$  conjugates of conjugation ratios 3, 2, 1, and 0.5 were loaded in wells 4, 5, 6, and 7, respectively. ALP- $\text{QD}_{557}$  and HRP- $\text{QD}_{557}$  were loaded in wells 9 and 11. (C) Native PAGE analysis of  $\text{QD}_{557}$  conjugates of SA. Standard SA was loaded on well 2, while SA- $\text{QD}_{557}$  conjugates of conjugation ratios 1, 0.5, 0.2, and 0.1 were loaded in wells 3, 4, 5, and 6, respectively, at 1  $\mu\text{g}$  SA/well. A duplicate set was loaded onto wells 8 through 12 at higher protein loading of 5  $\mu\text{g}$  SA/well. Standard  $\text{QD}_{557}$  was loaded on well 7.

Nanocrystal growth with the nucleation process is temperature dependent, wherein the precursors chemically transform into monomers to attain supersaturation and further atomic rearrangement.<sup>11</sup> CdTe QDs thus synthesized have shown convincing absorption and fluorescence properties (Figure 1S, Supporting Information). The presence of well-defined broad absorption spectra at shorter wavelength suggests the larger distances in the band gap of these particles. The shifts observed in the emission peak of thus-synthesized CdTe QDs were correlated to their size and in turn to the band gap energy of the particle. Thus, CdTe QDs having emission peaks at 523, 557, 576, and 601 nm with narrower full width at half-maximum (fwhm) in the range 45–70 nm and higher photoluminescence were synthesized at 100 °C in aqueous medium. Transmission electron microscopy (TEM) has determined the size of  $\text{QD}_{557}$  nanocrystal that is having a narrow size range of  $3 \pm 0.2$  nm with good dispersion in aqueous medium without any aggregation (Figure 1A).

Since QDs are synthesized from organometallic precursors, they have no intrinsic aqueous solubility. The native coordinating organic ligands on the surface of QDs must either be exchanged or functionalized with a ligand that can impart both solubility and potential bioconjugation sites.<sup>2</sup> Ligands that form a capping layer on the surface of the QDs must be biocompatible as biomolecules, and most of biological reactions are highly hydrophilic in nature. Therefore, MPA was used to stabilize the QDs that impart biocompatibility and necessary functional carboxylic groups for bioconjugation in aqueous media. CdTe QDs having emission peaks at 523, 557, 576, and 601 nm were conjugated to BSA, and  $\text{QD}_{557}$  was further conjugated with ALP, HRP, and SA separately by two-step EDC/NHS protocol, as  $\text{QD}_{557}$  has shown very prominent absorption and higher photoluminescence compared to other QD particles. The protein-conjugated samples have shown strong fluorescence when exposed to UV light (366 nm) after 2 h of incubation at 32 °C followed by dialysis to remove unconjugated QDs inferring retention of conjugated  $\text{QD}_{557}$ ,  $\text{QD}_{576}$ , and  $\text{QD}_{601}$ . However, conjugate samples with  $\text{QD}_{523}$  displayed no fluorescence under UV light.

Figure 1B,C represents native PAGE analysis of  $\text{QD}_{557}$  conjugated BSA, ALP, HRP, and SA. BSA- $\text{QD}_{557}$  conjugates of varying conjugation ratio (3:1, 2:1, 1:1, and 0.5:1) were observed

to have acquired greater mobility as compared to standard BSA. This can be ascribed to the increase in overall negative charge of the conjugates rendering them more mobility under electric field. Schroedter et al. (2002) has reported this property of nanoparticles to influence the charge density as a result of conjugation.<sup>12</sup> The increased molecular weight of conjugate was apparently overcome by the high negative charge and compactness of QD.<sup>13</sup> The observed drift in bands with an increase in conjugation ratio for BSA- $\text{QD}_{557}$  conjugates has suggested a greater density of QD per protein molecule. ALP conjugate also showed an observable drift. However, HRP conjugate developed a diffuse band due to enhancement of overall negative charge. The SA conjugates of varying conjugation ratio also showed a pattern similar to that of BSA conjugates. The standard QD can be observed to have moved along with the electrophoretic front due to its high mobility caused by small size and a high negative charge.

#### Effect of Bioconjugation on Photoabsorption Properties.

QD bioconjugates were subjected to photoabsorption studies to probe the changes in spectral behavior due to interactions of inorganic nanoparticles with biomolecules. Absorption spectra were taken for various protein conjugates of CdTe QDs. A remarkable change in the photoabsorption spectra was observed for all the protein bioconjugates of CdTe QDs. Protein bioconjugates of CdTe QDs such as  $\text{QD}_{523}$ ,  $\text{QD}_{557}$ ,  $\text{QD}_{576}$ ,  $\text{QD}_{601}$  conjugated to BSA, and  $\text{QD}_{557}$  conjugated to different proteins such as ALP, HRP, and SA displayed a remarkable deviation from their individual components in terms of their absorption spectra (Figure 2A,B and Supporting Information Figure 2S).

A new peak was observed in the 320–330 nm range, which was absent in the spectra of both QD and protein standards. The peak was absent when  $\text{QD}_{557}$  and BSA were simply mixed in the same ratio, suggesting absorption at 320–330 nm could be due to covalent conjugation of  $\text{QD}_{557}$  and BSA but not some electrostatic interactions among them. However, there was an enhancement of absorption at 280 nm, characteristic of a protein molecule and a slight depression of absorption from 200 to 270 nm for BSA- $\text{QD}_{557}$ , a region where QDs absorb strongly. Idowu et al. (2008) has reported the decrease of QD absorption due to conjugation with BSA.<sup>14</sup> Thus, the decrease in absorption of QD coupled to an increase in absorption of protein points toward coupling of the intrinsic energy states of two chromophores.

Absorption in the range 320–330 nm for QD–protein bioconjugates could be due to nonradiative dipole–dipole interaction among them. The intensity of absorption in the range 320–330 nm was found to correlate with percentage retention of QD from fluorescence data suggesting a link between absorption and the degree of conjugation. To probe this link, conjugations were performed varying the ratio between  $\text{QD}_{557}$  and BSA concentration. It was observed that absorption in the range 320–330 nm was gradually decreased with increase in BSA concentration (50, 100, 250, 500, 1000, 1500, 2000  $\mu\text{g/mL}$ ) during bioconjugation (Figure 2C). A maximum absorption was observed for 50  $\mu\text{g/mL}$  of BSA conjugated to  $\text{QD}_{557}$  (concentration of QD taken was 0.1 absorption unit at its excitation wavelength, 500 nm). Concomitantly, a gradual increase in absorption was observed when bioconjugation was done with increasing  $\text{QD}_{557}$  concentration at BSA concentration of 50  $\mu\text{g/mL}$  (Figure 2D).

Absorption was found to decrease logarithmically with the increase in ratio between  $\text{QD}_{557}$  and different protein concentration, wherein absorption was correlated with percentage

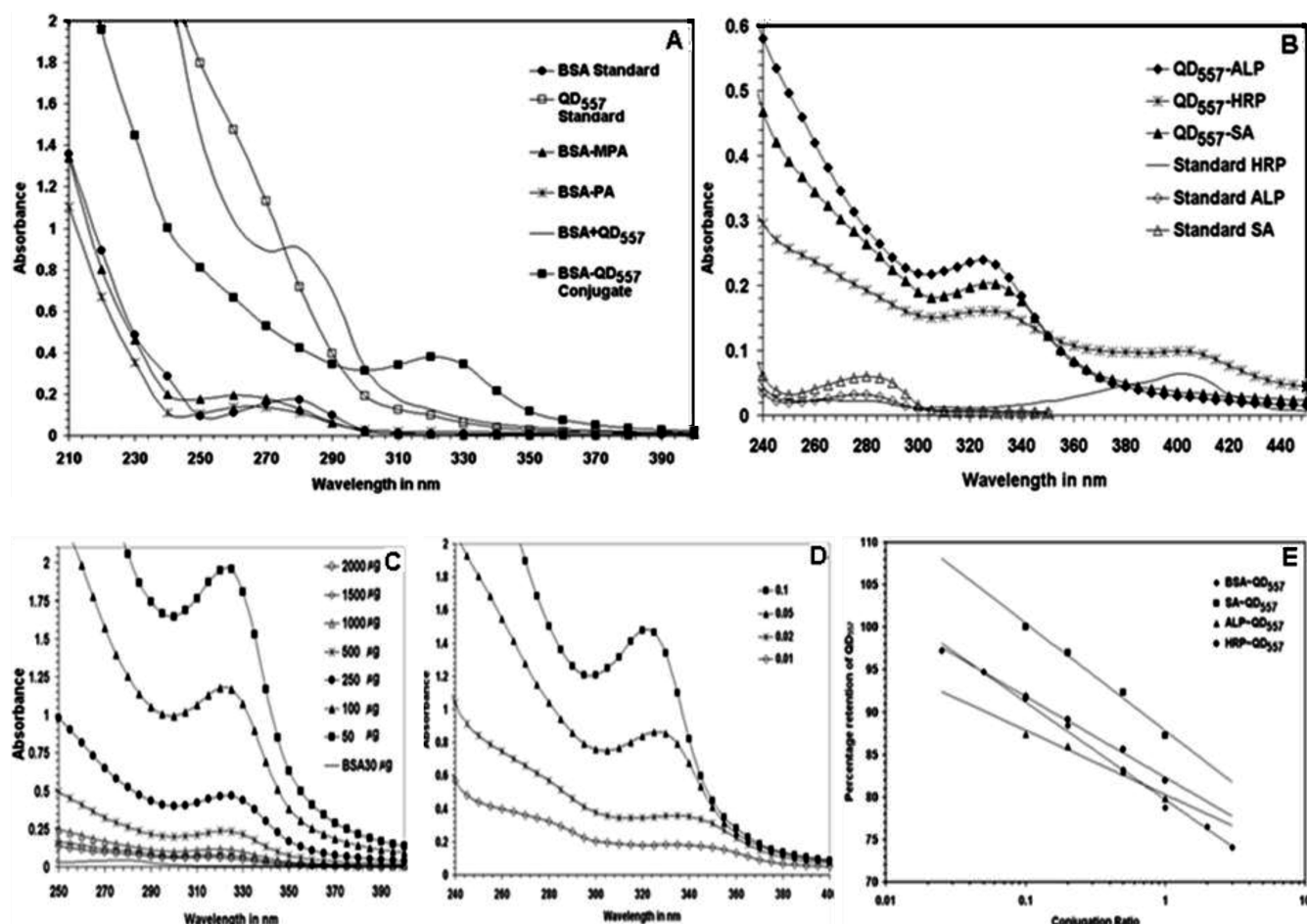


**Figure 2.** (A) Absorption spectra of BSA, CdTe QD<sub>557</sub> standard, MPA, PA, BSA-QD<sub>557</sub> conjugate, BSA-MPA conjugate, BSA-PA conjugate, and a mixture of BSA and QD<sub>557</sub> in the amounts present in the conjugate sample. (B) Absorption spectra of QD<sub>557</sub> conjugate with different proteins. (C) Variation of  $A_{330}$  for QD<sub>557</sub> conjugates with different BSA concentration. (D) Variation of  $A_{330}$  with different QD<sub>557</sub> concentration. (E) Variation of percentage retention of QD<sub>557</sub> with the conjugation ratio in four different QD<sub>557</sub>-protein bioconjugates from QD restricted absorbance spectrum. (QD<sub>557</sub>:protein is 1:0.025, 0.05, 0.1, 0.2, 0.5, 1, 2, and 3).

retention of QD<sub>557</sub> in the bioconjugates (Figure 2E). This suggests that absorption in the range 320–330 nm depends purely on the covalent attachment of protein to QD. Variation in slope can be attributed to the difference in percentage conjugation for different proteins. This further strengthens the above-mentioned hypothesis that absorption in the range 320–330 nm depends on covalent attachment of QD to protein alone. The occurrence of an absorption peak at 320–330 nm can thus be attributed to the effective coupling of the electronic orbitals of the conjugating entities. However, BSA-MPA and BSA-PA conjugates did not show any remarkable absorption in the range 320–330 nm that further confirms QD–biomolecular interactions (Figure 2A). Here, PA was used for conjugating BSA to ensure the absorption in the range 320–330 nm was not due to ligand binding which appeared in the presence of covalently conjugated CdTe QD. The deviation in optical behavior of protein-bioconjugated QD may be due to the formation of a possible protein shell on the surface of QD. Wang et al. (2006) have reported the use of denatured BSA to modify the surface of QDs to improve the chemical stability and photoluminescence. Further, Wang et al. (2006) have also reported a similar possibility when denatured BSA was used to modify the surface of CdTe QD.<sup>15</sup>

**CdTe-QD Retention and Fluorescence Quenching in Bioconjugates.** The fluorescence spectra were taken for QD-BSA conjugates (QD<sub>523</sub>, QD<sub>557</sub>, QD<sub>576</sub>, and QD<sub>601</sub>) restricting the protein concentration to 5 µg/mL for spectral analysis with excitation wavelength at 280, 320, and 350 nm separately. Fluorescence spectra gave a rough estimate of percentage retention of QD (Figure 3A). Additionally, blue shifts of 5 nm for QD<sub>557</sub>, 8 nm for QD<sub>576</sub>, and 13 nm for QD<sub>601</sub> were observed in the fluorescence spectra of QD after conjugation with BSA inferring a net reduction in Stokes shift of the conjugate. In addition, varying levels of fluorescence quenching were observed for BSA in QD<sub>523</sub>, QD<sub>557</sub>, QD<sub>576</sub>, and QD<sub>601</sub> conjugates (Figure 3B).

Further, it was observed that the percentage retention of QD and the percentage quenching of BSA fluorescence were proportionate to each other (Table 1). BSA–QD<sub>557</sub> conjugates have shown a red shift in the fluorescence peak of BSA with respect to conjugation ratio inferring solvent polarization effects on protein molecules due to the close proximity of QD (Figure 3S, Supporting Information). Generally, fluorescence spectra of proteins undergo a shift upon varying the polarity in the environment of aromatic amino acid residues as a result of binding of substrates, denaturation, and interactions with other

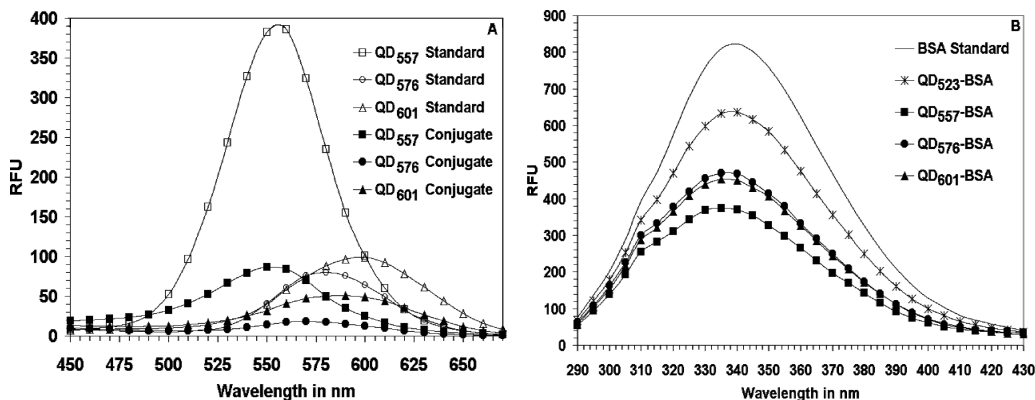


**Figure 3.** (A) Fluorescence spectra for standard QDs and their respective BSA conjugates. (B) Quenching of BSA fluorescence due to conjugation with various QDs.

**Table 1. Percentage Retention and Percentage Quenching for BSA Conjugates with Different QDs**

sample	percentage retention of QD (%)	percentage quenching of BSA fluorescence (%)
QD <sub>523</sub> -BSA	56.89	25.7
QD <sub>557</sub> -BSA	99.24	55.78
QD <sub>576</sub> -BSA	73.67	42.1
QD <sub>601</sub> -BSA	76.78	43.89

molecules.<sup>16</sup> A spectral blue shift of protein fluorescence may also occur due to the shielding of tryptophan residues from the hydrophilic environment.<sup>16</sup> Therefore, the red shift in protein fluorescence signifies the conformational changes induced by the interaction of QD and further exposure of tryptophan residues to the hydrophilic aqueous environment.<sup>17</sup> Generally, the tyrosine fluorescence ( $\lambda_{\text{max}}$  303 nm) is not significantly influenced by the environmental conditions.<sup>18</sup> Furthermore, there was an enhancement of QD<sub>557</sub> fluorescence at a higher ratio of QD<sub>557</sub> to BSA in the range 400–650 nm as observed in Figure 4A. The degree of fluorescence enhancement was increased with an increase in the energy of excitation. While excitation at 350 nm caused an enhancement of 100%, excitation at 280 nm caused 200% enhancement.

The enhancement of QD fluorescence upon bioconjugation was ascribed to the passivation of the QD surface by proteins against solvent effects in the aqueous media. Different proteins displayed various enhancement profiles as evident from Figure 4B. Idowu et al. (2008) have reported enhancement of QD emission in the presence of BSA, which signifies inhibition of nonradiative recombination of the surface vacancies.<sup>14</sup> Thus, a decrease in fluorescence emission of BSA after bioconjugation with CdTe QD<sub>557</sub> could be due to radiationless quenching and was found to be concentration-dependent. There was a linear decrease in BSA fluorescence with increasing concentration of CdTe QD after bioconjugation, suggesting an interaction between CdTe QD and BSA. Similar observations were made by Idowu et al. (2008), and it was reported that a progressive decrease in BSA fluorescence with increasing concentration of QD could be due to static and dynamic quenching together.<sup>14</sup> Fluorescence quenching as a result of the conjugation process may be due to energy transfer phenomena, excited-state reactions, or complex formation, which is referred to as static

quenching.<sup>19</sup> The appearance of a new absorption peak in the range 320–330 nm further confirms such nanobiomolecular interactions and suggests CdTe QD-BSA complex formation, which could be due to the formation of a possible protein shell on the surface of QD. As CdTe QD was synthesized in aqueous environment, there is a possibility of having certain trap sites on the surface of QDs. During CdTe QD-BSA complex formation, the formation of a possible protein shell on the surface of QD may eliminate nonradiative transitions. Further, the protein shell may passivate the surface of QDs, thereby inhibiting the radiationless recombination at the surface vacancies (Figure 5).<sup>19</sup>

**Photobleaching and Resonance Energy Transfer Phenomenon in CdTe QD Bioconjugates.** Several studies have demonstrated the effective use of QDs as FRET donors. FRET is a distance-dependent dipole–dipole interaction phenomenon of nonradiative transfer of excited-state energy from an excited donor molecule to an acceptor molecule. Generally, FRET may lead to a decrease in the fluorescence of donor chromophores and subsequent increase in the fluorescence of an acceptor chromophores.<sup>20</sup> QDs have been used to detect small analytes by utilizing a common strategy that relies on conjugating QDs to target binding receptors.<sup>7</sup> The QD conjugates are then exposed to appropriate acceptor-labeled target analogues, which are brought in close proximity to the QD by binding to the receptors. In this initial state, the QD-donor PL is quenched by efficient FRET to the proximal acceptor-labeled analogues. The presence of the target then displaces bound analogues from the surrounding conjugated receptors that can be detected through a reduction in FRET efficiency and a concomitant increase in PL of QD. The main limiting factor for QDs as FRET donors lies in their size, as FRET efficiency depends on center-to-center separation between donor and acceptor chromophores. Three variables contribute to overall QD donor size: core shell radius, coating, and bioconjugation. Therefore, successful QD FRET designs most often include very thin solubilization layers and direct attachment of bioreceptors to the QD surface to overcome this limiting factor.<sup>21</sup> Covalent conjugations between protein moiety and nanoparticles may lead to dipolar resonance interactions resembling Forster resonance energy transfer phenomenon.<sup>7,12,13</sup> CdTe QD has a broad excitation spectrum by virtue of its nature, and thus, it may be possible for CdTe QD to influence the optical properties of proteins as a result of covalent conjugation. This tightly bound covalent attachment between protein and CdTe QD has resulted in spatial closeness of the

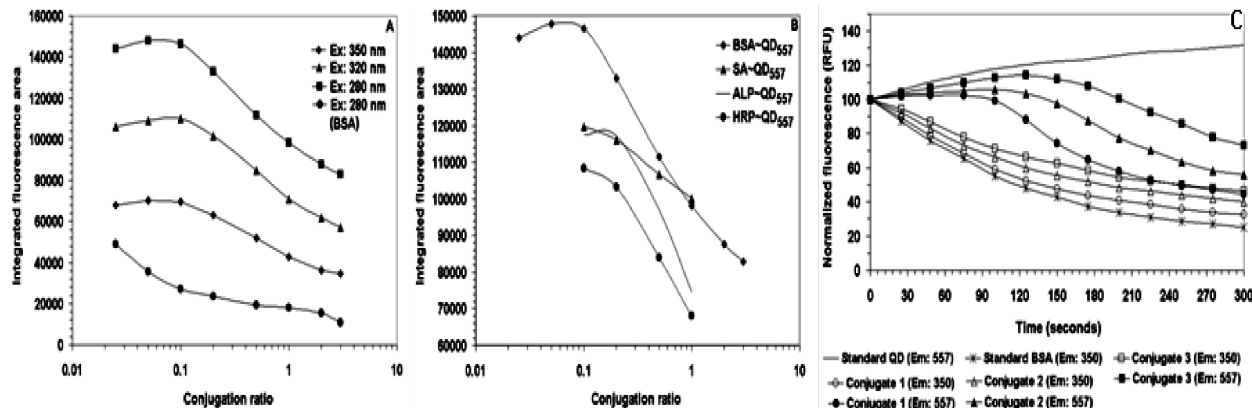


**Figure 4.** Variation in fluorescence emission spectra for protein–QD<sub>557</sub> bioconjugates proportional to the conjugation ratio. (A) Variation of integrated fluorescence area for BSA–QD<sub>557</sub> bioconjugates proportional to the conjugation ratios excited at three wavelengths: 280, 320, and 350 nm. The emission for QD component was collected from 450 to 650 nm, while that for the BSA component was collected in the 300–400 nm range. (B) Variation of integrated fluorescence area with conjugation ratio for QD<sub>557</sub> conjugates of BSA, SA, ALP, and HRP excited 280 nm. Emission for the QD component was collected from 450 to 650 nm. (C) Variation of normalized fluorescence over time for standard QD<sub>557</sub>, standard BSA, and BSA–QD<sub>557</sub> conjugates of three different ratios (conjugate 1 is BSA–QD<sub>557</sub> at 1:0.1, conjugate 2 is BSA–QD<sub>557</sub> at 1:1, and conjugate 3 is BSA–QD<sub>557</sub> at 1:3 ratio) from time course fluorescence spectra. The fluorescence of the BSA component was monitored at 350 nm, while that of the QD component was monitored at 530 nm.

molecules in the bioconjugate. Thus, covalent conjugation might have brought BSA and CdTe QD into such close proximity that has led to the appreciable spectral overlap between BSA and CdTe QD. This has resulted in the dipolar resonance interaction between BSA and CdTe QD as a donor–acceptor pair, respectively (Figure 5). This, in turn, might have allowed sufficient resonance energy transfer between BSA and CdTe QD in the BSA–QD<sub>557</sub> complex. FRET efficiency for various BSA–QD<sub>557</sub> conjugates were calculated by the following equation:<sup>22,23</sup>

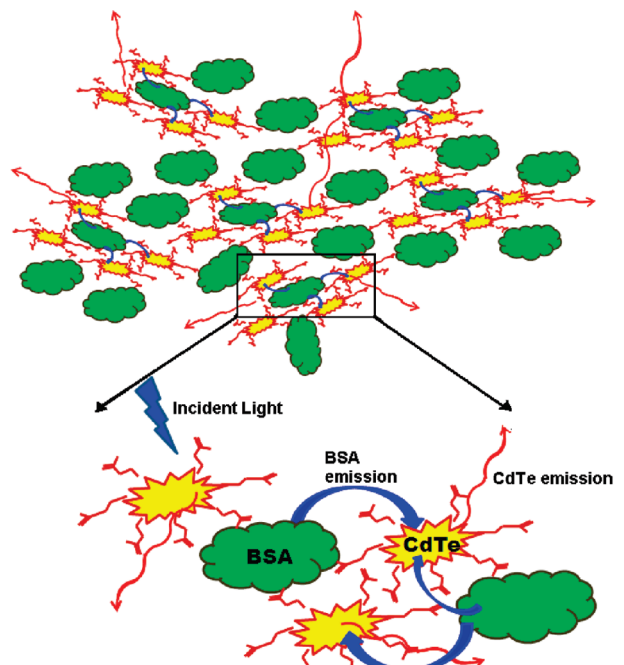
$$E = 1 - F_{da}/F_d \quad (1)$$

where  $F_{da}$  is the integrated BSA fluorescence in the presence of QD<sub>557</sub> and  $F_d$  is the integrated BSA fluorescence in the absence of QD<sub>557</sub>.

FRET efficiencies can also be inferred from the photobleaching rates of the donor in the presence and absence of an acceptor.<sup>24</sup> Photobleaching is the irreversible photochemical destruction of a fluorophore and always occurs from its excited state.<sup>22</sup> Resonance energy transfer from an excited donor to an acceptor fluorophore prevents the photobleaching of that donor fluorophore, and thus, high FRET efficiency leads to a longer photobleaching decay time constant. The energy transfer efficiency for BSA–QD<sub>557</sub> conjugate was determined by the following equation:<sup>22</sup>

$$E = 1 - \tau_{pb}'/\tau_{pb} \quad (2)$$

where  $\tau_{pb}'$  and  $\tau_{pb}$  are the photobleaching decay time constants of the donor in the presence and absence of the acceptor, respectively. The fact that time measurements are over seconds rather than nanoseconds makes measurement easier than fluorescence lifetime measurements, and because photobleaching decay rates do not generally depend on donor concentration, the careful control of concentrations needed for intensity measurements is not required. Time course fluorescence was obtained for standard QD<sub>557</sub>, standard BSA, and BSA–QD<sub>557</sub> conjugate samples excited at 280 nm. Fluorescence emission



Schematic representation of photo-absorption and resonance energy transfer in protein bioconjugated CdTe quantum dots

was monitored at 350 nm for the BSA component and 557 nm for the QD<sub>557</sub> component (Figure 4C).

The energy transfer efficiency for BSA–QD<sub>557</sub> conjugates was determined by making use of eq 1. Photobleaching lifetime was estimated for the BSA component by fitting the photobleaching curves to eq 2 (Table 2). Photobleaching-based calculation of FRET is based on the theory that the occurrence of resonance energy transfer reduces the fluorescence lifetime of the donor molecule, effectively protecting it against photobleaching.

**Table 2. Photobleaching Time ( $\tau_{pb}$ ) and FRET Efficiency (E) Determined for BSA–QD<sub>557</sub> Samples**

sample	photobleaching time (s)	E (%)
BSA	68.5	-
BSA–QD <sub>557</sub> (1:0.1)	82.6	17.11
BSA–QD <sub>557</sub> (1:1)	92.6	26.02
BSA–QD <sub>557</sub> (1:3)	106.4	35.61

Calculations of photobleaching FRET are based on the decreased rate of donor photobleaching relative to that measured for the donor in the absence of resonance energy transfer.

## ■ CONCLUSION

In summary, various optical and biological properties of CdTe–QD bioconjugates were characterized using absorption spectroscopy, fluorescence spectroscopy, and gel electrophoresis. Bioconjugation has significantly influenced the photoabsorption spectrum of QD–bioconjugates suggesting formation of a possible protein shell on the surface of QD. A proportionate quenching in BSA fluorescence with respect to conjugation ratio followed by an enhancement of QD fluorescence point toward possible nonradiative dipolar interactions between the two chromophores. Further, a reduction in photobleaching time for BSA as a result of bioconjugation with QD<sub>557</sub> supports the possibility of dipolar interactions, which are attributed to the nanobiomolecular interactions between CdTe–QD and tyrosine/tryptophan moieties of protein molecule. Thus, the initial experimental results suggest these bioconjugates can be considered as nanoparticle (NP) superstructures for the development of new-generation robust nanoprobes.

## ■ ASSOCIATED CONTENT

**S Supporting Information.** Absorption and emission spectra of QDs synthesized by aqueous method and spectrum showing quenching of BSA fluorescence for BSA–QD<sub>557</sub> conjugates. This material is available free of charge via the Internet at <http://pubs.acs.org>.

## ■ AUTHOR INFORMATION

### Corresponding Author

\*M. S. Thakur, Ph.D. Senior scientist, Fermentation Technology & Bioengineering Department, Central Food Technological Research Institute, Mysore-570020, India. E-mail: msthakur@cftri.res.in, msthakur@yahoo.com.

## ■ ACKNOWLEDGMENT

The authors gratefully acknowledge the Director, CFTRI, and CSIR for providing necessary laboratory facilities. Mr. A. C. Vinayaka is thankful to CSIR for providing research fellowship. Dr. Sanjukta Patra, IIT, Ghati is greatly acknowledged for kind help and support. Authors also thank Aeronautical Development Agency (ADA), Bangalore, for providing the required financial support for this project under National Programme on Micro and Smart Systems (NPMASS) scheme.

## ■ REFERENCES

- (1) Bao, H., Gong, Y., Li, Z., and Gao, M. (2004) Enhancement effect of illumination on the photoluminescence of water soluble CdTe nanocrystals: Towards highly fluorescent CdTe/CDs core shell structure. *Chem. Mater.* 16, 3853–3859.
- (2) Sapsford, K., Pons, T., Medintz, I. L., and Mattoussi, H. (2006) Biosensing with luminescent semiconductor quantum dots. *Sensors* 6, 925–953.
- (3) Vinayaka, A. C., Basheer, S., and Thakur, M. S. (2009) Bioconjugation of CdTe quantum dot for the detection of 2,4-D by competitive fluoroimmunoassay based biosensor. *Biosens. Bioelectron.* 24, 1615–1620.
- (4) Chouhan, R. S., Vinayaka, A. C., and Thakur, M. S. (2010) Thiol-stabilized luminescent CdTe quantum dot as biological fluorescent probe for sensitive detection of methyl parathion by a fluoroimmuno-chromatographic technique. *Anal. Bioanal. Chem.* 397, 1467–1475.
- (5) Chen, Q., Ma, Q., Wan, Y., Su, X., Lin, Z., and Jin, Q. (2005) Studies on fluorescence resonance energy transfer between dyes and water-soluble quantum dots. *Luminescence* 20, 251–255.
- (6) Wang, J. H. (2007) Fluorescence resonance energy transfer between FITC and water-soluble CdSe/ZnS quantum dots. *Colloids Surf. A* 30, 168–173.
- (7) Vinayaka, A. C., and Thakur, M. S. (2010) Focus on quantum dots as potential fluorescent probes for monitoring food toxicants and foodborne pathogens. *Anal. Bioanal. Chem.* 397, 1445–1455.
- (8) Clapp, A. R., Medintz, I. L., Uyeda, H. T., Fisher, B. R., Goldman, E. R., Bawendi, M. G., and Mattoussi, H. (2005) Quantum dot-based multiplexed fluorescence resonance energy transfer. *J. Am. Chem. Soc.* 127, 18212–18221.
- (9) Li, M., Ge, Y., Chen, Q., Xu, S., Wang, N., and Zhang, X. (2007) Hydrothermal synthesis of highly luminescent CdTe quantum dots by adjusting precursors' concentration and their conjunction with BSA as biological fluorescent probes. *Talanta* 72, 89–94.
- (10) Hermanson, G. T., Mallia, A. K., Smith, P. K. (1992) *Immobilized Affinity Ligand Techniques*, pp 53–98, Academic Press, San Diego.
- (11) Mahler, B., Spinicelli, P., Buil, S., Quelin, X., Hermier, J. P., and Dubertret, B. (2008) *Nat. Mater.* 7, 659–664.
- (12) Schroedter, A., Weller, H., Eritja, R., Ford, W. E., and Wessels, J. M. (2002) Biofunctionalization of silica-coated CdTe and gold nanoparticles. *Nano Lett.* 2, 1363–1367.
- (13) Mamedova, N. N., Kotov, N. A., Rogach, A. L., and Studer, J. (2001) Protein–CdTe nanoparticle conjugates: preparation, structure and interunit energy transfer. *Nano Lett.* 1, 281–286.
- (14) Idowu, M., Lamprecht, E., and Nyokong, T. (2008) Interaction of water-soluble thiol capped CdTe quantum dots and bovine serum albumin. *J. Photochem. Photobiol. A: Chem.* 198, 7–12.
- (15) Wang, Q., Kuo, Y., Wang, Y., Shin, G., Ruengruglikit, C., and Huang, Q. (2006) Luminescent properties of water-soluble denatured bovine serum albumin-coated CdTe quantum dots. *J. Phys. Chem. B* 110, 16860–16866.
- (16) Güney, O., Saraç, A. S., and Mustafaev, M. (1997) Fluorescence and turbidimetry study of complexation of human serum albumin with polycations. *J. Biact. Compat. Polym.* 12, 231–244.
- (17) Tian, J., Liu, J., Hu, Z., and Chen, X. (2005) Binding of the scutellarin to albumin using tryptophan fluorescence quenching, CD and FT-IR spectra. *Am. J. Immunol.* 1, 21–23.
- (18) Ruan, K., Li, J., Liang, R., Xu, C., Yu, Y., Lange, R., and Balny, C. (2002) A rare protein fluorescence behavior where the emission is dominated by tyrosine: case of the 33-kDa protein from spinach photosystem II. *Biochem. Biophys. Res. Commun.* 293, 593–597.
- (19) Liu, P., Wang, Q., and Li, X. (2009) Studies on CdSe/L-cysteine quantum dots synthesized in aqueous solution for biological labeling. *J. Phys. Chem. C* 113, 7670–7676.
- (20) Förster, T. (1948) Zwischenmolekulare energiewanderung und fluoreszenz. *Annalen. Physik.* 6, 55–75.
- (21) Goldman, E. R., Anderson, G. P., Tran, P. T., Mattoussi, H., Charles, P. T., and Mauro, J. M. (2002) Conjugation of luminescent

quantum dots with antibodies using an engineered adaptor protein to provide new reagents for fluoroimmunoassays. *Anal. Chem.* 74, 841–847.

(22) Patel, R. C., Lange, D. C., and Patela, Y. C. (2002) Photo-bleaching fluorescence resonance energy transfer reveals ligand-induced oligomer formation of human somatostatin receptor subtypes. *Methods* 27, 340–348.

(23) Chong, E. Z., Matthews, D. R., Summers, H. D., Njoh, K. L., Errington, R. J., and Smith, P. J. (2007) Development of FRET-based assays in the far-red using CdTe quantum dots. *J. Biomed. Biotechnol.* 2007, 1–7.

(24) Wang, L., Chen, T., Qu, J., and Wei, X. (2010) Photobleaching-based quantitative analysis of fluorescence resonance energy transfer inside single living cell. *J. Fluoresc.* 20, 27–35.